

SIZE EFFECTS IN THE BIAxIAL TENSILE-COMPRESSIVE BEHAVIOUR OF CONCRETE: PHYSICAL MECHANISMS AND MODELLING

P. Rossi and F.-J. Ulm,
Laboratoire Central des Ponts et Chaussées, Paris, France

Abstract

This paper analyses failure mechanisms and apparent size effects in the biaxial tensile-compressive behaviour of concrete. To this end, a probabilistic discrete crack model is used, to determine numerically failure surfaces in the tensile-tensile and tensile-compressive loading range, on account of size effects considered as volume effects. The results (failure-mechanisms, crack-patterns, volume effects, etc.) are discussed in some details with respect to the loading state applied. Size effects on the failure surface are quantified in terms of stress-invariant ratios at peak load for 8 loading paths. It is found that size effects decrease with the hydrostatic pressure increasing, i.e. when passing from the tensile loading range into the tensile-compressive range. This can be explained by the activation of friction at the crack lips in a stable crack propagation, which regularizes mechanical volume effects, and thus apparent size effects.

1 Introduction

Size effects in the tensile behaviour of concrete are well studied (see, for a review, Bazant, 1991). Less is known about these effects when passing from the simple or biaxial tension domain into the biaxial tensile-compressive range. In return, most of the loading states of concrete structures lie in this domain, whence the importance to ascertain the knowledge and to seek for quantifying size effects in this loading range. Furthermore, this domain is of great importance for continuous models of concrete cracking (plasticity, damage etc.), which require material parameters on the failure surface in this domain.

This paper analysis failure mechanisms and apparent size effects in the biaxial traction-compressive behaviour of concrete. To this end, a probabilistic discret crack model is used, to determine numerically failure surfaces in the tensile-tensile and tensile-compressive loading range, on account of size effects considered as volume effects. The results (failure-mechanisms, crack-patterns, volume effects, etc.) are discussed in some details with respect to the loading state applied. Some assumptions concerning the physical mechanisms which can explain this difference with respect to the loading range are then proposed. These assumptions seem coherent with the numerical results obtained.

2 Probabilistic modelling of concrete cracking

Cracking of concrete is strongly influenced by the heterogeneity of the matter: the tensile strength of concrete is mainly related to that of the cement paste, which -in turn- is governed by the presence of voids, microcracks etc. created during the concrete hardening by non-uniform shrinkage during hydration at the scale of the heterogeneous material, i.e. at the scale of the concrete aggregates. This heterogeneity of the matter constituting concrete can be considered to be at the basis of apparent size effects, governing the overall cracking behaviour at the macroscopic scale of material observation (i.e., scale of laboratory test-specimen). This has led to the development of the *probabilistic modelling of concrete cracking* over the last decade (Rossi and Wu, 1992). It belongs to the family of statistically based deterministic models using the finite-element method. It accounts for cracks as geometrical discontinuities (discrete crack approach), and for the heterogeneity of the matter by random distribution functions with experimentally determined mean values, $m(f_t)$ and $m(E)$, and standard deviations, $s(f_t)$ and $s(E)$, of tensile strength f_t

and Young's modulus E , respectively. For their experimental determination, a major experimental research has been performed at the LCPC, which has led to the proposing of analytical expressions of the distribution functions, (Rossi et al., 1994a), with merely knowledge of

1. the apparent compressive strength f_c of the concrete determined by a standardized test on a cylinder 16 cm in diameter and 32 cm high,
2. the ratio of the volume of concrete V_t to the volume of the coarsest grain V_g .

In the finite element analysis, these functions are used by replacing in the experimental determined distribution function the volume of the test specimen V_t by the volume of each singular solid finite element. This is consistent with physical evidence: the smaller the scale of observation (respectively the modelling scale) with respect to that of the structure, the larger the fluctuation of the local mechanical characteristics, and thus the (modelled) heterogeneity of the matter. This renders the numerical results mesh-independent (Rossi and Guerrier, 1994). With respect to the local and probabilistic character of the approach, the volume of the solid mesh elements must be sufficiently small with respect to the volume of the modelled structure, so that the probabilistic analysis performed on the scale of the mesh element is representative with respect to the structure.

The cracks are modelled using special contact elements that interface the solid elements. A crack (i.e. a contact element) "opens" (appearance of a geometrical discontinuity) when the stress normal to a fracture plane $\sigma_N = \mathbf{n} \cdot \boldsymbol{\sigma} \cdot \mathbf{n}$ reaches the local tensile strength f_t randomly distributed, thus:

$$\sigma_N - f_t \leq 0 \quad (1)$$

Crack criterion (1) refers to the fact that concrete cracking corresponds to a mode-I mechanism, in tension as well as in compression. In the latter failure occurs due to the appearance of oblique cracks (Torrenti et al., 1993). The failure mechanisms in compression and the consequences on the modelling scales are discussed in some details in Rossi et al. (1994b). The oblique cracks are created locally by tensile stresses. In order to capture this failure mechanism in terms of modelled heterogeneity, the modelling scale has to be small with respect to the "structural" scale at which the failure occurs (small columns created by vertical cracks within the sample), much smaller than that of the sample. At a scale above, this oblique cracking appears as a shear failure and in the limit of a

homogeneous material, no tensile stresses occur in the material under compression (see figure 1). Hence, relative to the modelled heterogeneity in the analysis, a shear-crack criterion may be necessary, reading in its simplest form:

$$|\tau| - c \leq 0 \quad (2)$$

where $\tau = \mathbf{t} \cdot \boldsymbol{\sigma} \cdot \mathbf{n}$ is the shear stress and c is the local cohesion of the material. Since this crack-criterion reflects a mode-I criterion at a modelling scale below, cohesion c cannot be regarded as an independent material characteristic - in contrast to the tensile strength f_t . In fact, since the oblique cracks open once the tensile stress reaches the local tensile strength, cohesion c is related to the tensile strength, such that:

$$c = \gamma f_t \quad (3)$$

where γ is a coefficient of proportionality, assumed constant. This assumption implies that the coefficient of proportionality is independent of size effects and allows for its determination from experimental data, ($\gamma = c / f_t \approx 5$, see Rossi et al., 1994b). With crack opening local tensile strength f_t and cohesion c are set to zero, and remain zero throughout the calculation (local irreversible fragile tensile behaviour). In other words, the strength is not recovered when the crack recloses, and only normal compression stresses are admissible. The friction between the two edges of the geometrical discontinuity created (edges of the crack) is taken into account by a cohesionless Mohr-Coulomb criterion reading:

$$|\tau| - \sigma_N \operatorname{tg} \varphi \leq 0 \quad (4)$$

With respect to the local irreversible fragile tensile behaviour, friction is only activated when the element re-closes after opening. Note that an angle of friction $\varphi = 45^\circ$ represents sufficiently the experimentally observed non-linear behaviour in the peak-load and post-peak load range in compression (Rossi et al., 1994b).

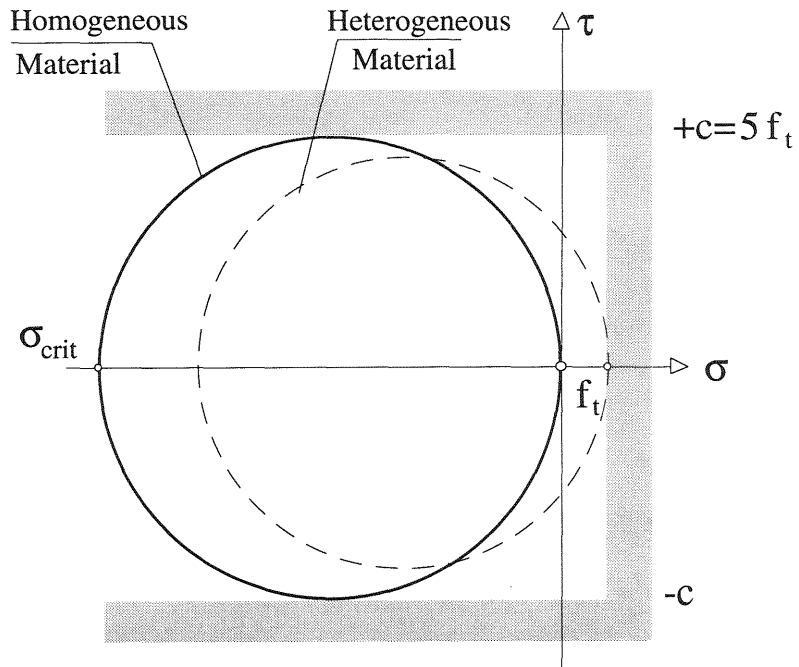


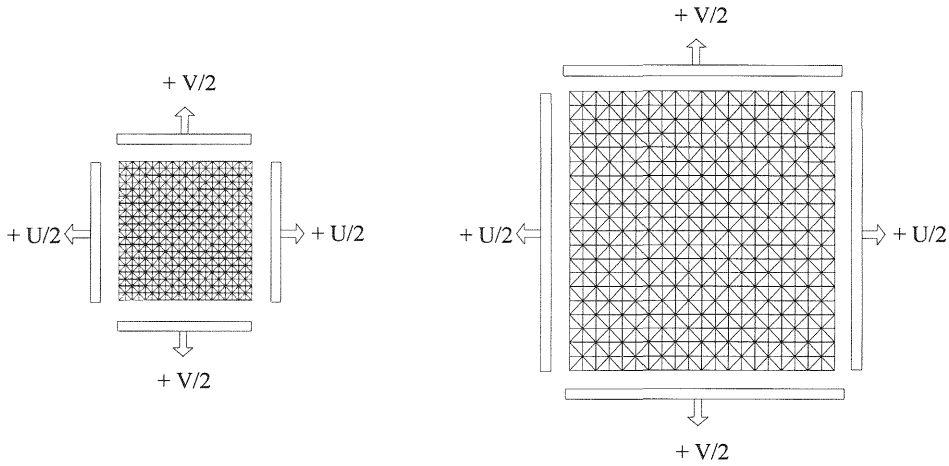
Figure 1: Mohr stress plane with different admissible stress states at different modelling scales of the heterogeneous material

3 Size effects in the failure behaviour of concrete

In order to show the importance of size effects in the tensile-compressive range, the failure surfaces for a concrete of a compressive strength of $f_c = 30\text{MPa}$ are determined on two prismatic test-specimen sizes of $15/15/5\text{ cm}$ and $30/30/10\text{ cm}$, having thus a volume ratio of $V_2/V_1=8$, with V_1 =volume of test specimen 1 and V_2 =volume of test specimen 2. The choice of the (*numerical*) test specimen sizes was inspired by the size of test specimen $20/20/5$ used by Kupfer et al. (1969), whose (*experimental*) data are considered as reference.

3.1 (Numerical) loading-program, boundary conditions, input data

Like in laboratory test experience a loading program and clear boundary conditions need to be defined: for each test-specimen size 8 loading paths are applied, to determine 8 points on the failure surface in the tension-tension and tension-compression range. Furthermore, for each loading path 10 calculations with a Monte-Carlo procedure (permutations) are performed, in order to be for each loading condition representative in a statistical sense. The (numerical) tests are displacement driven, under



Test-specimen 1 (15/15/5 cm) Test-specimen 2 (30/30/10 cm)
 Figure 2: FE-meshes with boundary conditions

Table 1. (Numerical) test program
 (* 0 displacement imposed means stress free boundary conditions)

U/V	Tensile domain			Compressive-tensile domain				
	1/1	2/1	0*/1	-1/1	-2/1	-3/1	-4/1	-1/0*

plane stress conditions, with displacements U and V imposed in the x and y direction at the boundary as illustrated figure 2, according to the test-program, summarized in table 1. The finite element meshes are shown in figure 2, having the same number of elements for both specimen sizes. Hence, the scale of observation (i.e. the scale of modelled heterogeneity) with respect to the specimen size is kept constant, which renders the results mesh-independent.

The following input data required in the probabilistic model are applied:

- Cylinder compressive strength $f_c = 30 \text{ MPa}$
- Mean Young modulus $E = 30000 \text{ MPa}$
- Maximum aggregate size (diameter) $\phi = 10 \text{ mm}$
- Angle of friction $\varphi = 45^\circ$
- Ratio cohesion/tensile resistance $\gamma = c / f_t = 5$

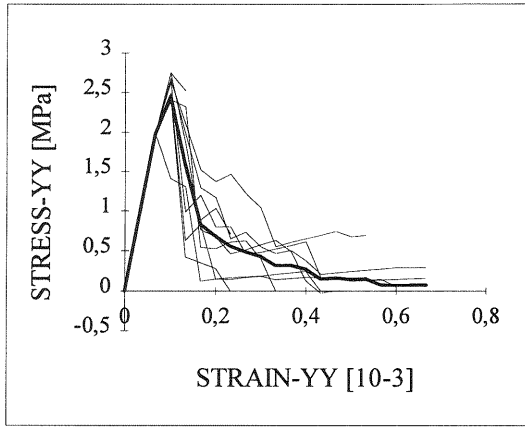
3.2 Stress-strain curves: mean values, scattering, crack pattern

The results are explored in the standard manner as experimental results, i.e. stresses from the reaction-forces at the boundary where displacements are imposed, and strains from the displacements imposed. Figures 3, 4

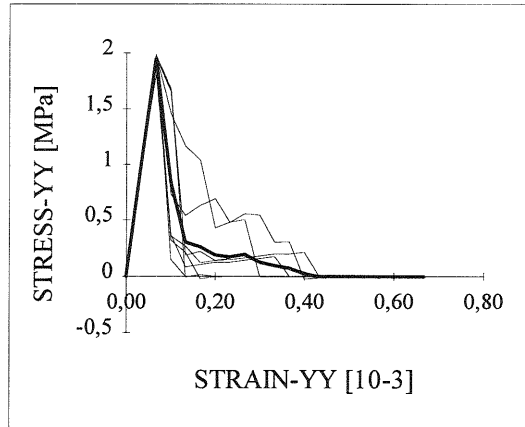
and 5 show some stress-strain relations so obtained for the two test-specimen. The results can be analysed in terms of stochastic scattering: a mean curve (bold) and the scattering for 10 different simulations obtained by Monte Carlo permutation. A comparison of figures 3, 4 and 5 shows that the scattering of the peak value is the more pronounced the smaller the volume of the test-specimen, in particular in the tensile domain (figure 3: uniaxial tension), while the scattering decreases for both test-specimens (i.e. decreasing volume effects) when passing from the tensile into the compressive-tensile loading range (figure 4: $U/V=-1/1$, $\sigma_1 / \sigma_3 \approx -0,85$ at peak load; figure 5: $U/V=-2/1$, $\sigma_1 / \sigma_3 \approx -0,3$ at peak load).

It is noteworthy, that under the imposed displacement conditions, stress- and strain-state are co-axial and correspond to the principal stresses and strains up to the peak values of a loading path, while diverging strongly from this co-axiality in the post-peak range under combined compressive-traction loading due to shear effects. Hence, in this range, the softening load-displacement or stress-strain curves should be handled with care (for instance when exploring them in terms of fracture energy, dissipated energy, continuous softening models etc.). More precisely, when performing a displacement-driven biaxial compression-tension test, whether experimentally or numerically, the permanent (or plastic) dilatation of the material due to cracking may become greater than the traction displacement imposed at the boundary. The latter then blocks the (intrinsic) dilatation of the material which gives rise to apparent ductile effects in the softening range, which are not intrinsic to the material but induced by boundary conditions (see figure 5, as well as Torrenti et al., 1993).

Finally, some crack-patterns obtained in the numerical simulations are shown in figure 6. They are similar for the two-test specimen sizes, differ however from one probabilistic simulation to the other performed on the same test specimen size under identical loading conditions, due to different random distributions of the material properties within the test-specimen.

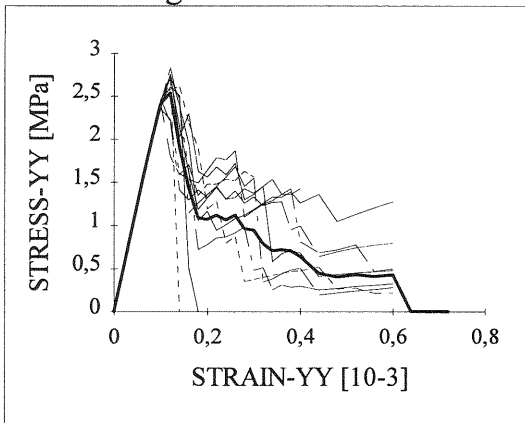


Test-specimen 1: 15/15/5

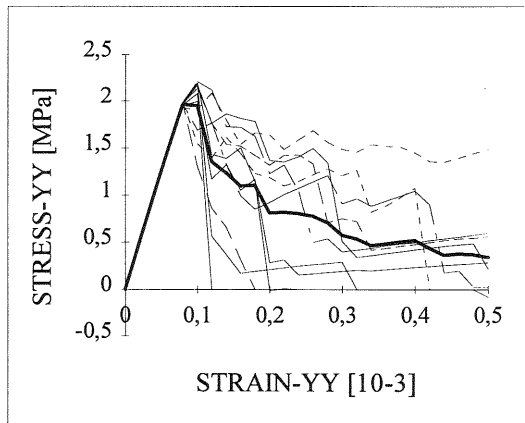


Test-specimen 2: 30/30/10

Figure 3: Uniaxial tension stress-strain curves for $U/V=0/1$



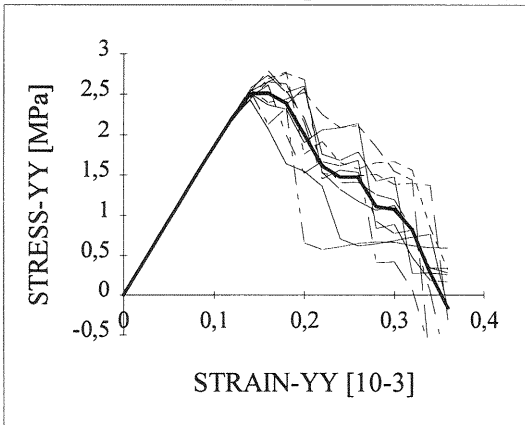
Test-specimen 1: 15/15/5



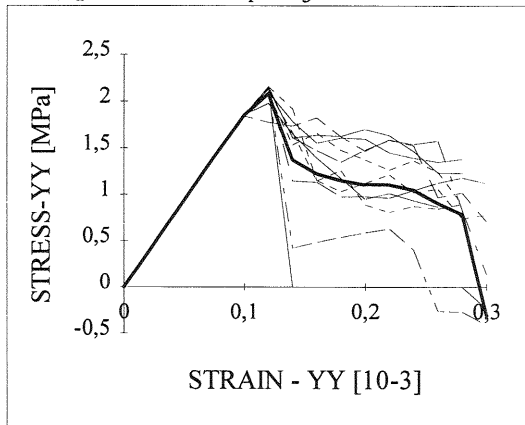
Test-specimen 2: 30/30/10

Figure 4: Compression-Tension stress-strain curves for $U/V=-1/1$

Ratio of principal stresses at (tensile) peak load: $\sigma_1 / \sigma_3 \approx -0,85$



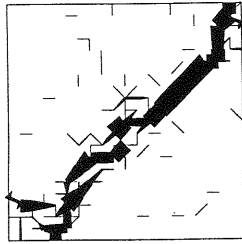
Test-specimen 1: 15/15/5



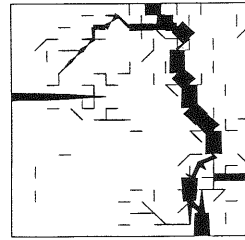
Test-specimen 2: 30/30/10

Figure 5: Compression-Tension stress-strain curves for $U/V=-2/1$

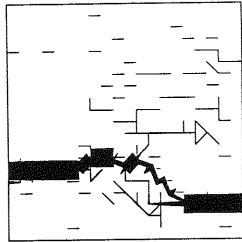
Ratio of principal stresses at (tensile) peak load: $\sigma_1 / \sigma_3 \approx -0,3$



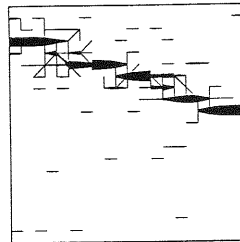
$U/V = 1/1$: Biaxial tension



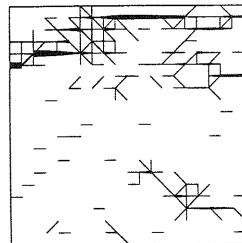
$U/V = 2/1$: Biaxial tension



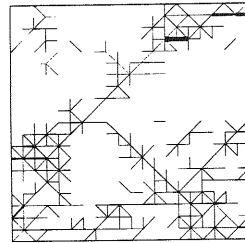
$U/V = 0/1$: Uniaxial tension



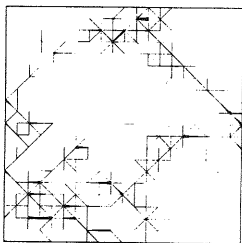
$U/V = -1/1$: Compression-tension



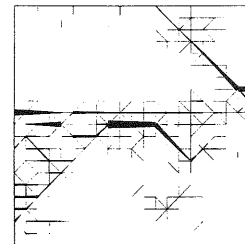
$U/V = -2/1$: Compression-tension



$U/V = -3/1$: Compression-tension



$U/V = -4/1$: Compression-tension



$U/V = -1/0$: Uniaxial Compression

Figure 6: Examples of crack patterns for different loading conditions

3.3 Size effects on the failure surface

For each volume size 80 (numerical) tests were performed, which allow to determine 8 loading points on the failure surface for the two test-specimen sizes in the tensile-tensile and compressive tensile range, of which each one corresponds to the mean value of 10 tests carried out (summarized in table 2). We explore them here in the classical manner in the principal stress space $\sigma_I \times \sigma_{II}$ for plane stress conditions ($\sigma_{III} = 0$), as shown in figure 7. The curves so obtained perfectly correlate in form and shape with experimental results found in literature (e.g. Kupfer et al., 1969), but show however non-negligible size effects. More precisely, since the material up to the peak load can be considered as isotropic, the failure surface can be represented in terms of stress invariants, namely, the first invariant of stress tensor σ (the mean stress σ), the second deviator invariant τ and the Lode angle θ , defined by

$$\sigma = \text{tr}\sigma / 3 \quad \tau = \sqrt{\frac{1}{2}\mathbf{s}:\mathbf{s}} \quad \cos\theta = \frac{2\sigma_1 - \sigma_2 - \sigma_3}{\sqrt{12}\tau} \quad (5)$$

with $\mathbf{s} = \sigma - \sigma\mathbf{1}$ the stress deviator tensor. The values for these three invariants for the different loading paths and test-specimen-sizes are given in table 2. Furthermore, we may seek to quantify size effects in terms of the ratio of stress invariants, as calculated in table 2:

$$\rho(\sigma) = \frac{\sigma(V1)}{\sigma(V2)} \quad \rho(\tau) = \frac{\tau(V1)}{\tau(V2)} \quad (6)$$

Thus, for a volume-ratio of $V2/V1=8$ we find a size effect in terms of stress invariant ratios $\rho(\sigma) \approx \rho(\tau)$ of about 25% in the tensile domain, which reduces to about 15% in the compressive range, i.e. with confinement pressure increasing. In other words, size effects are the higher, the lower the hydrostatic pressure. This dependency reflects the pressure dependence of the failure behaviour of concrete.

Finally, note that the compressive strength obtained numerically for the prismatic test-specimens ($f_{cp-V1} = 21,12\text{MPa}$ and $f_{cp-V2} = 18,16\text{MPa}$) is smaller than the cylinder compressive strength $f_c = 30\text{MPa}$ used as input data. This can be explained by the well known "shape effect": the compressive strength obtained on a cylinder is associated with a complex failure mechanism of oriented slippage planes confined in three dimensions (e.g. Torrenti et al., 1991), while the compressive strength obtained on prismatic test-specimens corresponds to two dimensional slippage planes under plane stress conditions.

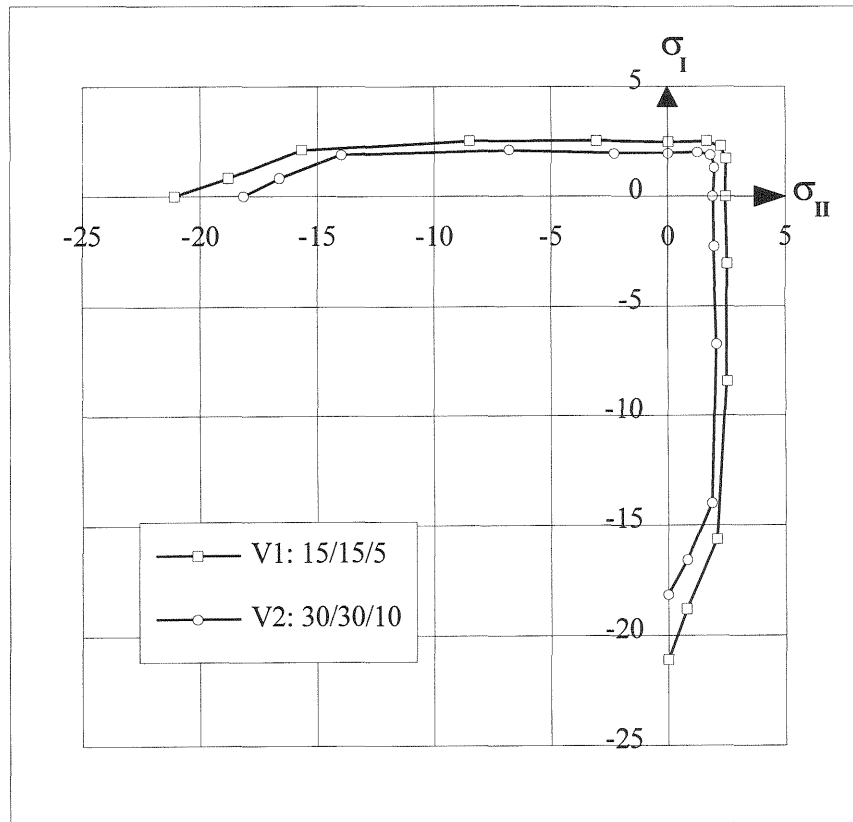


Figure 7: Failure surfaces for the two test-specimen sizes

Table 2. Principal stresses and invariants at the failure surface in [MPa]

U/V	Tensile domain			Compressive-tensile domain				
	1/1	2/1	0/1	-1/1	-2/1	-3/1	-4/1	-1/0
σ_{I-V1}	2,24	2,50	0	-3,08	-8,47	-15,67	-18,81	-21,12
σ_{II-V1}	2,25	1,67	2,46	2,54	2,51	2,08	0,80	0
σ_{I-V2}	1,84	2,01	0	-2,31	-6,77	-13,99	-16,58	-18,16
σ_{II-V2}	1,85	1,30	1,95	-1,96	2,08	1,88	0,83	0
$\sigma(V1)$	1,50	1,39	0,82	-0,18	-1,99	-4,53	-6,00	-7,04
$\tau(V1)$	1,30	1,27	1,42	2,81	5,75	9,71	11,10	12,20
$\theta(V1)$	60°	41°	0°	33°	47°	54°	58°	60°
$\sigma(V2)$	1,23	1,10	0,65	-0,12	-1,56	-4,04	-5,25	-6,05
$\tau(V2)$	1,07	1,02	1,13	2,13	4,63	8,67	9,82	10,49
$\theta(V2)$	60°	40°	0°	33°	47°	54°	58°	60°
$\rho(\sigma)$	1,22	1,26	1,26	1,55	1,27	1,12	1,14	1,16
$\rho(\tau)$	1,22	1,25	1,26	1,32	1,24	1,12	1,13	1,16

In return, the ratio of tensile over compressive strength obtained on the same test-specimen (in size and shape) respects the standard ratio of about 8-10 % experimentally established for normal strength concretes, and seems independent of volume effects.

4 Physical mechanisms explaining size effects in biaxial loadings

As stated just before, *apparent* size effects can be related to the *apparent* pressure dependence of the failure behaviour of concrete, as well known and as generally applied in the constitutive modelling of (continuous) concrete behaviour (e.g. Chen, 1982). Hence, the physical origin of size effects may be sought for in the physical origin of this apparent pressure dependence. The latter is merely due to friction forces at the crack lips in the heterogeneous material (Acker et al., 1987), which stabilize the crack propagation when activated during loading. In other words, friction forces activated at the crack lips necessarily correspond to a stable crack propagation, since it allows for the dissipation of usefull mechanical work into heat form. The higher the hydrostatic pressure, the more energy can be dissipated via friction at the crack lips into heat form in a stable crack propagation. In return, unstable cracks bring about failure, and are thus related to the macro-material strength (nominal strength at the level of laboratory test specimen). More precisely, if the mechanical loading applied leads direct to an unstable crack propagation with little friction forces activated at the crack-lips, the occurrence of failure is directly related to the number of initial defaults (voids, microcracks, etc.) in the matrix, denoted N_{id} , created during the concrete hardening by non-uniform shrinkage at the level of the heterogeneous material. The macro-material strength is then governed by these initial defaults actived during loading (derived from Weibull's theory (1939)). The (nominal) strength thus decreases with N_{id} increasing in the specimen, while it decreases with the volume of material decreasing. This mechanical "volume effect" is the more pronounced, the lower the hydrostatic pressure, and thus the activation of friction forces, and *vice versa*. In other words, friction forces at the crack-lips (and thus dissipation of effective mechanical work into heat form!), regularize volume effects, and thus apparent size effects. This may explain the pressure dependence of size effects on the (nominal) failure surface. Finally, the pressure dependence of size effects via friction forces at the crack lips is consistent with the well known fact, that an apparent ductile behaviour of concrete is due to friction phenomena activated in the cracks, and that volume effects decrease when the mechanical behaviour becomes more ductile.

5 Conclusions

This paper is concerned with physical mechanisms and modelling of apparent size effects in the tensile compressive loading range of concrete. It is worthwhile to recall the approach used for quantifying size effects in this domain:

In a first step loading surfaces for different test-specimen sizes are determined. To this end, -and in alternative to an experimental approach- a probabilistic discrete crack model is applied, which accounts for cracking as geometrical discontinuities, which merely open in mode I, i.e. once the stress normal to a fracture plane reaches the randomly distributed local tensile stress. This numerical model is able to capture well the failure mechanisms of concrete in this loading range in terms of crack creation and propagation on account of size effects, considered as volume effects, as well as the nominal strengths of the test specimens under 8 different loading paths. From these calculations, the failure surfaces of two concrete test-specimens having a volume ratio of $V_2/V_1=8$ are determined. In order to quantify size effects, the results are explored in terms of stress-invariant ratios of the two test-specimen sizes at peak load. It is found that size effects decrease with hydrostatic pressure increasing. This reflects the apparent pressure dependence of the failure behaviour of brittle materials like concrete. This pressure dependence of size effects can be explained by friction forces activated at the crack lips associated with a stable crack propagation, which regularize mechanical volume effects, and thus apparent size effects. This analysis seems coherent with the (numerical) test-results obtained in the biaxial tensile-compressive loading range. They need now to be confirmed in the biaxial compression-compression range and under triaxial stress conditions, which -with respect to the crack patterns- involves necessarily three-dimensional numerical simulations.

Finally, the importance of size effects in the failure behaviour of concrete complicates the constitutive modelling of concrete behaviour based upon the concept of a representative elementary volume (i.e. continuous models like plasticity, damage etc.). In fact this concept implies the existence of a scale defining the dimensions of the elementary volume. This scale is not intrinsic to the matter, but necessarily imposed by the scale of material observation which -in turn- involves non-negligible size effects. Here, a continuous constitutive model that respects the scale of observation with respect to the scale of application needs still to be designed.

6 References

- Acker, P., Boulay, C. and Rossi, P. (1987) On the importance of initial stresses in concrete and of the resulting mechanical effects. **Cem. & Concr. Res.**, 17, 755-764.
- Bazant, Z. P., Editor (1991) **Fracture Mechanics of Concrete Structures**. Proc., FraMCoS1, Elsevier, London.
- Chen, W.F. (1982) **Plasticity in reinforced concrete**. McGraw-Hill Inc.
- Kupfer, H., Hilsdorf, H.K., and Rusch, H. (1969) Behaviour of concrete under biaxial stresses. **ACI Journal**, 66(8), 656-666.
- Rossi, P., and Wu, X. (1992) Probabilistic model for material behaviour analysis and appraisalment of concrete structures. **Mag. Concr. Res.**, 44, No. 161, 271-280.
- Rossi, P., and Guerrier, F. (1994) Application of a probabilistic discrete cracking model for concrete structures, in **Fracture and Damage in quasibrittle structures: experiment, modelling and computer analysis** (eds Z.P. Bazant et al.), E. & F.N. Spon, 303-309.
- Rossi, P., Wu, X., Le Maou, F., and Belloc, A. (1994a) Scale effect on concrete in tension. **Materials and Structures**, 27, 437-444.
- Rossi, P., Ulm, F.-J., and Hachi, F. (1994b) Compressive behaviour of concrete: physical mechanisms and modelling. Submitted for publication to **J. Engng. Mech, ASCE**.
- Torrenti, J.M., Desrues, J.M., Benajja, E.H. and Boulay,C. (1991) Stereophotogrammetry: a mean of visualizing strain localization in concrete under compression. **J. Engng. Mech., ASCE**, 117(7), 1455-1465.
- Torrenti, J.M., Benajja, E.H. and Boulay,C. (1993) Influence of boundary conditions on strain softening in concrete compression test. **J. Engng. Mech., ASCE**, 119(12), 2369-2384.